Scientific paper

Design of "Turn-Off" Fluorescent Nanoprobe for Highly Sensitive Detection of Uric Acid using Green Synthesized Nitrogen-Doped Graphene Quantum Dots

Sopan Nangare,[1] Shweta Baviskar,[2] Ashwini Patil[3] and Pravin Patil[2,*]

[1] *Department of Pharmaceutics, H. R. Patel Institute of Pharmaceutical Education and Research, Shirpur-425405, Dist: Dhule, Maharashtra state, INDIA-425405*

[2] *Department of Pharmaceutical Chemistry, H. R. Patel Institute of Pharmaceutical Education and Research, Shirpur-425405, Dist: Dhule, Maharashtra state, INDIA-425405*

[3] *Department of Microbiology, R. C. Patel Arts, Science, and Commerce College, Shirpur, Dist: Dhule, Maharashtra state, INDIA-425405*

** Corresponding author: E-mail: rxpatilpravin@yahoo.co.in*

Received: 02-24-2022

Abstract

Green synthesized graphene quantum dots (GQD) have been doped with nitrogen in an attempt to boost their optical characteristics and application sectors. In the present investigation, the blue luminescent nitrogen-doped GQDs (N-GQDs) were synthesized by single-step hydrothermal synthesis using tamarind shell powder as a precursor. The particle size and zeta potential of N-GQDs were found to be 11.40 nm and be –35.53 mV, respectively. A quantum yield as high as 23.78 % was accomplished at an excitation wavelength of 330 nm at neutral pH. It gets quenched sensitively in the existence of uric acid (UA) combining static quenching, electron transfer, and an inner filter effect mechanism. A linear range was obtained for UA from 10 μM to 100 μM, with a limit of detection (LOD) of 401.72 ± 0.04 pM. Additionally, the N-GQDs were selective toward UA in presence of metal ions and biomolecules that indicated its impending use to monitor UA in clinical samples. In conclusion, this work demonstrates that the N-GQDs as a sensing probe for UA recognition with notable advantages including socioeconomic, simple, and less time-consuming methods as compared to other methods. In the future, it can be potentially explored as a biosensor for UA detection in clinical samples.

Keywords: Graphene Quantum Dots; N-GQDs; Uric acid; Biosensor; Tamarind Shell Powder

1. Introduction

Principally, UA (2.6,8-trihydroxypurine) is the primary product of purine synthesis.[1] As per literature, in the general population, UA is referred to between 0.13 mM to 0.46 mM and 2.49 mM to 4.46 mM in serum and urine, respectively.[2] As we know, the abnormal levels of such metabolites in body fluids can cause several diseases.[3] Plentiful literature revealed that the increased UA levels in body samples are indicative of hypertension, gout, cardiovascular disease, kidney disease, high cholesterol, and many more.[4] In comparison, low concentrations of UA are also connected with multiple sclerosis and oxidative stress.[5,6] In diagnosis and healthcare, it is crucial to quantify metabolites in blood or other biological samples. Therefore, a rapid, responsive, precise, and cheap method of assessment must be developed to track such metabolites in body fluids including serum and urine.[5]

Literature survey reported that electrochemical sensing,[7] a colorimetric method,[8] a chromatographic method,[9] etc. are currently engaged detection techniques for UA in different body fluid samples. However, some in-conveniences such as complicated synthesis or challenging extraction, advanced equipment, expensive and tedious limiting their practical uses, are present in these approaches.[5] There are no exceptions for benefit of fluorescence. It is highly sensitive, and it shows a fast reaction, and operative simplicity in contrast to the oth-

er existing approaches.[5, 10] From the last decades, ample reports have been reported for the detection of UA using fluorescent nanomaterials. Ding *et al.,* designed the graphene oxide-based carbon quantum dots (CQDs) as an electrochemical sensor for detection UA.[11] In another study, CQDs- hybrid composites-based electrochemical sensor has been constructed by Abbas and colleagues for recognition of UA.[12] Currently, application of GQDs as a sensing material is gaining much consideration from research fraternities. Thanks to its tunable photoluminescence properties GQDs have created substantial interest as a potential new class of carbon-based, luminescent nanomaterials.[10] The growing advancement in fluorescent sensors and bioimaging has been growing for the GQD because of their high bio-compatibility and photostability.[13,14] Applications of GQDs in UA sensing a redox modulated fluorescent strategy for a finding of UA and glucose using fluorescent GQDs based probe has been reported.[5] Kunpatee and co-authors reported the detection of UA using GQDs mediated ionic liquid modified screen-printed carbon electrode that offers the 0.03 μM of lowest detection limit.[15] However, the QY of GQDs mentioned is far lower than traditional quantum dots (QDs), which restricts QD's wide-ranging use for different purposes. Hence, the improvement of QYs has become one of the obstacles to the use of GQDs. Several scholars have successfully shown that GQDs can be reliably transformed into an amino-functionalized GQD or π-conjugated system employing doping of heteroatoms.[14] As per literature, doping is an efficient method to alter the electronic density of bulk semiconductor materials. Besides, it helps to tune the optical and electrical properties. Recently, nitrogen doping in graphene structure enabled the in-plane substitution of nitrogen atoms to graphene as an *n*-type semiconductor.[16] Therefore, in this work we developed the doped GQDs as fluorescent nanomaterials.

Nitrogen doping is a feasible approach for altering the electrical, chemical, and structural functions of GQDs to boost their efficiency in sensing applications.[17] Li and co-authors found, owing to the intense electron-withdrawing outcome of the doped 'N' atom, that the as-prepared N-GQDs have special optoelectronic properties.[18] Besides, a potential mechanism for tuning GQDs fluorescent properties via the charge transfer effect of the functional group was suggested by the Chattopadhyay group.[19] Due to the high QY and superb bleaching resistance of fluorescent materials, many research groups have been used N-GQDs as fluorescent sensors for sensing biological small macromolecules, organic small molecules, and metal or non-metal ions.[20] It is intended, by adjusting the surface characteristics and the associated fluorescent property, the design of realistic sensors for the assessment of UA in the urine can be promising. In the meantime, N-GQDs normally have greater amounts of QY than GQDs and are good for the fluorescence study in spiked real-time body fluid (urine). A preference of methods has been developed for the N-GQDs preparation including hydrothermal method,[21] direct electrolysis,[22] pyrolysis,[23] etc. using different chemicals as a precursor. Additionally, owing to the costly facilities, complex and time-consuming processes, the aforementioned protocols are unconvincing.

In this study, we illustrate a single step, relatively inexpensive and environmentally safe in preparing N-doped GQDs through hydrothermal treatment of Tamarind seed as a green source. We present a new kind of fluorescent sensor for UA detection based on the fluorescence Turn On-Off strategy. The synthesized N-GQDs show a high quantity of QY and emit light blue luminescence. Interestingly, owing to the stronger electrostatic interaction and electron transfer between blue luminescent N-GQDs and UA, the photoluminescence intensity of the N-GQDs could be quenched efficiently (Scheme 1). Finally, based

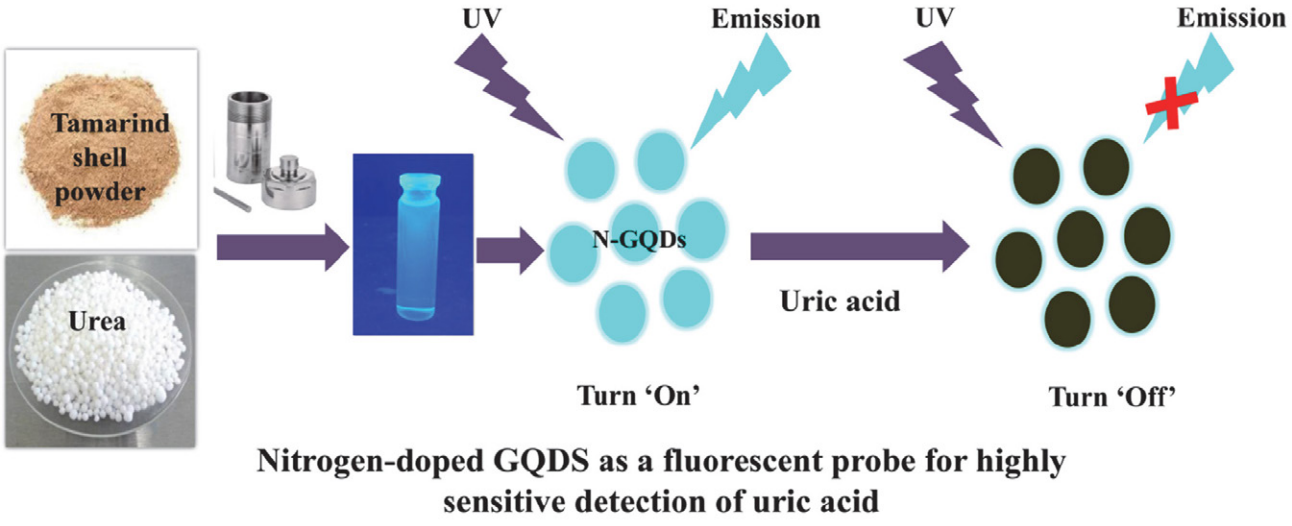

Scheme 1: One spot synthesis of N-GQDs using tamarind shell powder and sensing of UA

on a finding of the proposed N-GQDs fluorescent sensor, it could be an exceptional alternative as high sensitivity and selectivity for UA recognition.

2. Materials and Methods

2. 1. Materials

Uric acid (2, 6, 8-trihydroxypurine, ≥99%) and urea (≥99%) were purchased from Sigma-Aldrich. The sodium hydroxide, sodium chloride, calcium chloride, glycine, glucose, sucrose, lysine, alanine, quinine sulfate were collected from Lobachemie, Chemicals. Pvt. Ltd. Mumbai, India. All chemicals plus reagents utilized for synthesis and characterization of N-GQDs were of analytical grade (AR) and applied as received without purification. Double distilled water (DDW) was prepared in the laboratory. Tamarind seed was collected from the local market of Shirpur, Maharashtra (India).

2. 2. Methods

2. 2. 1. Processing of Tamarind Shell

In the beginning, 0.5 kg of tamarind shell (Tamarindus indica) waste was collected from the local market, Shirpur city (Dhule, Maharashtra). Further, the tamarind shell waste was dried using a laboratory hot air oven. The temperature was programmed at 60 °C and then decreased to 40 °C at the rate of –0.14 °C/minutes for 12 h. After drying, the dried shells were checked for stuck dirty materials on the shells. Finally, shells were crushed into tiny pieces via a mortar pestle. Further, the obtained powder was subjected to grinding to obtain fine tamarind shell powder.

2. 2. 2. Synthesis of N-GQDs

The N-GQDs synthesis from Tamarind shell powder and urea was achieved through the one-pot hydrothermal method. Briefly, 500 mg of fine tamarind shell powder was dispersed in 20 mL of double-distilled water (DDW) followed by 20 minutes of sonication. After that, 100 mg urea was added to the above dispersion. Finally, the prepared dispersion was transferred into a Teflon-lined autoclave in a stainless-steel hydrothermal reactor in a hot air oven at 200 °C for 8 h. After the end of the hydrothermal process, the resultant solution was kept to bath sonication for 20 minutes at 25 °C, which gives uniform dispersion of N-GQDs. For purification purposes, the obtained N-GQDs were shifted to the dialysis (for 24 h) using a dialysis bag (12,000 kDa, 0.22 μm), which help to remove the insoluble carbon materials. Afterward, the final dialyzed solution was transferred to centrifugation (Refrigerated Centrifuge, Elteck Overseas Pvt. India) at 9000 rpm for 20 minutes (4 °C to 10 °C) to remove the impurities.

2. 2. 3. Freeze-Drying of N-GQDs

In this study, liquid N-GQDs solution was processed for lyophilization by using a laboratory freeze dryer (Freezone12, Labconco, MO, USA). Briefly, the N-GQDs solution was pre-freeze at –30 °C for 36 h at the laboratory deep freezer (Southern Scientific Lab Instrument, India). After that, the primary drying of N-GQDs was performed at –53 °C and 0.016 mBar for 24 h. Afterward, the secondary drying of N-GQDs was performed at 10 °C for 8 h and was followed by drying at 25 °C for 4 h with a steady increase in temperature at 1 °C/min. Finally, the temperature of the cold trap was maintained at –53 °C until the end of the drying process.

2. 2. 4. Characterizations of N-GQDs

The synthesized N-GQDs were characterized by the UV-visible spectra was recorded between 800 to 400 nm on UV–vis spectrophotometer (UV 1800 Shimadzu, Japan) using a quartz cuvette. FT-IR spectra of N-GQD were recorded using an FT-IR spectrophotometer (Agilent CARY 630 FT-IR) at 4 cm^{-1} resolution in the absorption area of 4000 to 1000 cm^{-1}. Energy Dispersive X-ray Spectroscopy (EDAX) was used to provide qualitative and quantitative surface analysis. The particle size of synthesized N-GQDs was measured via Nanoplus 3 Particulate System (Micromeritics, USA). The green synthesized N-GQDs shape, size, and crystalline nature were obtained using HR-TEM (HR-TEM, Jeol/JEM 2100) with a LaB6 light source at 200 kV. The fluorescence study of N-GQDs was performed using a UV chamber (details) at different wavelengths such as 254 nm and 365 nm along with visible light.

2. 2. 5. pH Influence Study

The pH of the N-GQDs solution actively affects the fluorescence properties of the N-GQDs since the pH affects the surface stability and molecularity of the surface functional groups. The prepared N-GQDs were subjected to different pH ranges from 1 to 12 to study the pH dependant changes in the fluorescence intensity.[24] Herein, different predefined pH such as 1, 3, 7, 9, and 12 of N-GQDs solution was adjusted using 1.5 M solution of sodium hydroxide and 0.5 M hydrochloric acid at room temperature. Then, the pH value of the N-GQDs solution was recorded using a digital pH meter, and solutions were kept aside for 60 min. After that, the fluorescence intensity was recorded at excitation 330 nm and corresponding changes in the intensities were recorded.

2. 2. 6. Quantum Yield (QY)

In this study, the 'QY' of the N-GQDs was calculated by using a comparative method. Quinine sulfate was dissolved in 0.1 M sulphuric acid (φ_{st} = 54%) as a standard for QY determination. Then, the dilutions were prepared

using double distilled water (DDW). The absorbance was measured at 350 nm via a UV-Vis spectrophotometer and optical density values were kept below 0.1 to reduce the re-absorption effect. Fluorescence emission spectra of quinine sulfate, as well as N-GQDs, were recorded at 350 nm excitation and a graph was plotted for integrated fluorescence intensity against absorbance. The 'QY' of N-GQDs was calculated using the following equation,

$$\varphi_x = \varphi_{st}\left(\frac{Grad_x}{Grad_{st}}\right)\left(\frac{\eta_x}{\eta_{st}}\right)$$

wherein, 'φ' is representing the QY. The subscripts 'x' and 'st' represent test (N-GQDs) and standard (quinine sulfate) respectively. Grad is the slope of fluorescence intensity *vs.* absorbance plot. The 'η' is the refractive index of the solvent.

2. 2. 7. Uric Acid-Sensing Study

Detection of UA was carried out by using a spectrofluorometer (JASCO FP8200 spectrofluorometer) at neutral pH. Initially, 2 mL of synthesized N-GQDs solution were taken in a quartz cuvette and excited at 330 nm with a slit width of 5 nm for both excitations as well as emission wavelength at a scanning range of 335 nm to 520 nm at room temperature. To study the sensitivity of N-GQDs for UA detection, different concentrations of UA from 10 μM to 1000 μM were incorporated into an aqueous solution of N-GQDs (2 mL) and uniformly shaken followed by 5 minutes of incubation time at controlled room temperature (25 °C). Afterward, fluorescence intensities were measured in triplicate for more accuracy. Notably, N-GQDs probe fluorescence intensity and the concentration of UA were found to have a linear function as the calibration curve. Different analytical characteristics including the limit of detection and the limit of quantification were calculated using slope and standard deviation. Moreover, the precision of the proposed sensing method was measured as interday and intraday variations.

2. 2. 8. Interference Study

The selectivity of N-GQDs (2 mL) was analyzed against a range of metal ions and biomolecules. For the interference study, an aliquot of the stock solutions of non-target samples namely, Na^+, K^+, Ca^+, Ag^+, bovine serum albumin, lysine, glycine, alanine, glucose, sucrose, lactose, ascorbic acid, etc. were prepared in DDW (pH 7). A concentration of 100 μM was chosen for all the metal ions and biomolecules for interference study. Briefly, the 1 mL of N-GQDs solution was mixed with 500 μL of these interfering substance solutions, separately. After 10 minutes, the fluorescence intensity of all samples was recorded at 330 nm (excitation wavelength) with 5.0 nm silt width for both excitation and emission wavelength. In addition, the mixture of all metal ions and biomolecules with UA (sample A) was investigated to confirm the interference of foreign substances in the UA sample. The repeatability of N-GQDs was measured by the proposed method using 30 μM of UA samples (n = 6).

3. Results and Discussion

3. 1. Characterization of N-GQDs

In the present study, the applicability of N-GQDs as a fluorescent nanomaterial belonging to the 'C' family was explored for the recognition of UA in aqueous media. Briefly, a one-step, facile and eco-friendly method was preferred to synthesize N-GQDs using tamarind shell powder in a Teflon-lined hydrothermal stainless-steel autoclave reactor. Accordingly, the tamarind shell was proved to be an efficient and reliable waste material for synthesizing of GQDs while urea successfully donated nitrogen for the doping of nitrogen on the GQD structure. Inside the reactor, under high pressure and temperature conditions, tamarind shell powder forms the primary graphitic frame, and the nitrogen atoms were doped onto the graphitic structure. The synthesis procedure was optimized by altering the precursor's concentration as well as by changing the reaction time. The various batches were thus synthesized. As a result, it displayed momentous variation in the fluorescence properties. From these results; the final optimized parameters were identified for the synthesis of N-GQDs. Briefly, the fluorescence spectra were recorded at a fixed and varying wavelength to measure the excitation-dependent behavior. The synthesized N-GQDs were obtained in liquid form and then subjected to the different wavelengths in a UV- cabinet for fluorescence study. The solution of synthesized N-GQDs was looking pale yellow (or brownish) in visible light (Figure 1A). When a solution was transferred to the UV light excitation wavelength 254 nm, green fluorescence was observed (Figure 1B). In the case of UV light excitation wavelength 365 nm, the bright blue fluorescence of N-GQDs was obtained.[25] The varied colors observed in N-GQDs fluorescence were most possibly caused by solvent attachment/ different emissive traps of 'N' on green synthesized GQDs surface.[26] The oxygen-rich group provides the blue shift in photoluminescence emission from N-GQDs. Moreover, 'N' contains a strong electron affinity that offers the photoluminescence blue shift.[18]

For further investigation of optical properties of green synthesized GQDs, the UV-vis absorption spectra and fluorescence spectra were recorded. Figure 1D depicted the typical absorption peak at 229 nm that confirmed establishment of the graphitic structure of N-GQDs. It shows the absorption peak of N-GQDs in water at 200 nm to 800 nm against DDW (as a blank). The UV visible spectra of synthesized N-GQDs showed a maximum absorption peak at ~235 nm due to the π-π* transition of C=C. The shoulder peak at ~344 nm is due to n-π* transitions of

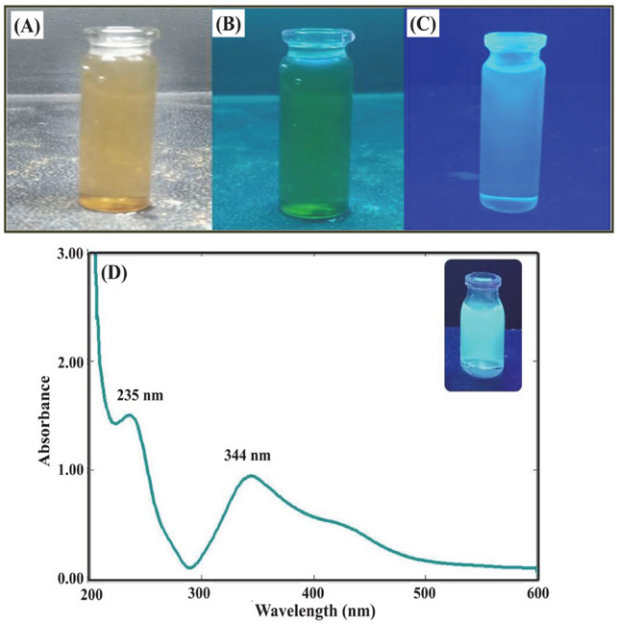

Figure 1: A) N-GQDs in Visible Light, (B) N-GQDs excited in UV light wavelength 254 nm, (C) N-GQDs excited in UV light wavelength 365 nm, (D) UV-Visible spectra of N-GQDs

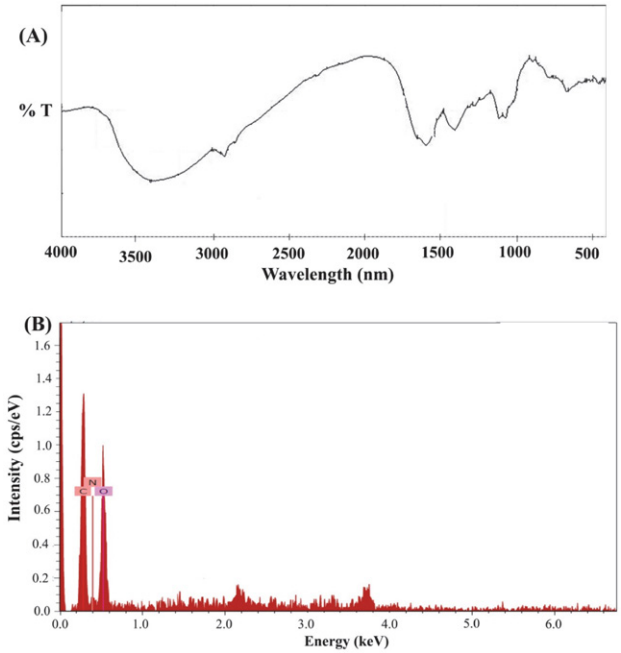

Figure 2: (A) FT-IR Spectra of N-GQDs, (B) EDAX spectra of N-GQDs

C=O.[27] Herein, these two absorption peaks confirmed that there is a certain absorption peak in N-GQDs. In conclusion, it confirmed the green synthesis of N-GQDs using the hydrothermal method.[20, 25]

FT-IR was used to characterize the presence of major functional groups in synthesized N-GQDs (Figure 2A). The FT-IR spectrum of N-GQDs showed the absorption peak of the stretching vibration of the –OH group at 3412.0 cm^{-1} whereas the strong absorption peak 3230 cm^{-1} can vibrate of amine (NH_2) bond. The overlapping of –OH and NH_2 was obtained due to the aqueous form of N-GQDs. Moreover, the peak at 1408.0 cm^{-1} can be attributed to the bimodal bending vibration of –NH. The C-N stretching vibration was obtained at 1276.92 cm^{-1}. Accordingly, it confirms the chemical interaction between the 'N' source and carboxyl. Moreover, it assures the existence of N on green synthesized GQDs surface.[25] The vibration peaks at 1658.84 cm^{-1}, 1120.68 cm^{-1}, and 1026.16 cm^{-1} can be ascribed to C=O stretching, C–O stretching, and C–O bending, respectively. In conclusion, the different functional

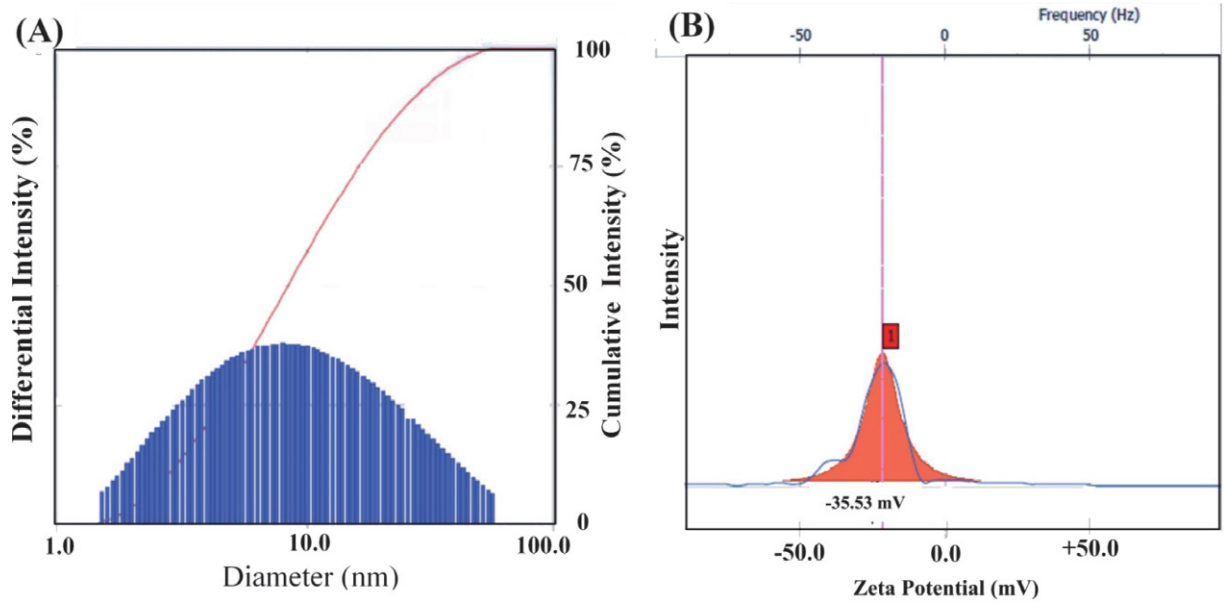

Figure 3: Particle size analysis (A) and zeta potential (B) of green synthesized N-GQDs

groups including –OH, –NH, and –COOH on N-GQDs surface confirmed the hydrophilicity and stability of the N-GQDs in an aqueous system.[23]

The elemental analysis of synthesized N-GQDs was conducted for authentication of the occurrence of C, O, and N (Figure 2B) elements. In brief, it provides the details of wt.% of these mentioned elements in synthesized N-GQDs from green precursors. Herein, the presence of C, O, and N was found to be 41.09 wt%, 49.00 wt%, and 9.91 wt% respectively. Therefore, the existence of these elements demonstrates the successful formation of the N-GQDs.[28] Moreover, the confirmation of the amide group in N-GQDs can form the hydrogen bonds between water molecules and N-GQDs, which helps to improve the water solubility of prepared N-GQDs.[20] It is worthy to mention that particle size is the foremost critical factor since particle size is a potential technique for confirming the transformation of a micro-sized structure to a nano-sized structure. In this study, the particle size of green synthesized N-GQDs was found to be 12.6 ± 11.1 nm that confirming the synthesis of nanosized N-GQDs (Figure 3A). The polydispersity index (PDI) was found to be 0.35 ± 0.09. It assured that the prepared N-GQDs exhibited uniform distribution in media. The zeta potential of N-GQDs was checked to confirm the surface charge as well as stability. The zeta potential of N-GQDs was found to be –35.53 mV (Figure 3B), which assures that the prepared N-GQDs exhibited good stability.

The morphological features of purified N-GQDs were characterized using HR-TEM. As depicted in Figure 3A, the GQDs are small, rounded, and uniformly dispersed with an average particle of size 7 nm. Moreover, the typical lattice spacing was found to be 0.23 nm demonstrating a graphitic structure of green synthesized N-GQDs. Figure 3B showed the selected area diffraction (SAED) pattern of N-GQDs that assured the crystalline nature of N-GQDs. In conclusion, it confirmed the successful synthesis of nanosized N-GQDs.[20]

3. 2. pH-Dependent Fluorescence Study of N-GQDs

Nitrogen doping is a feasible approach for altering the electrical, chemical, and structural functions of GQDs to boost their efficiency in sensing applications. The synthesized N-GQDs solution was excited at different excitation wavelengths from 300 to 400 nm length, with an increment of 10 nm, slit width is 5 nm and scanning range is 315–525 nm at 25 °C (Figure 5A). The N-GQDs showed the emission at 400 nm when excited from 300 nm to 330 nm and the emission peak was decreased and shifted towards the longer wavelength when excited from 340 nm to 400 nm. The strongest emission peak was obtained at 400 nm when excited at 330 nm. In this study, the emission spectrum of the N-GQDs was showed excitation-dependent PL behavior. Literature survey reported that the shift in emission peak positions with different excitation wavelengths is depending on several key factors such as quantum confinement effect, size effect, elemental composition, edge states, surface functional groups, conjugated π-domains, and defects in the carbon framework.[10] The effect of pH on synthesized N-GQDs was also studied by fluorescence spectroscopy. The fluorescence intensity of N-GQDs at different pH was shown in Figure 5B. The syn-

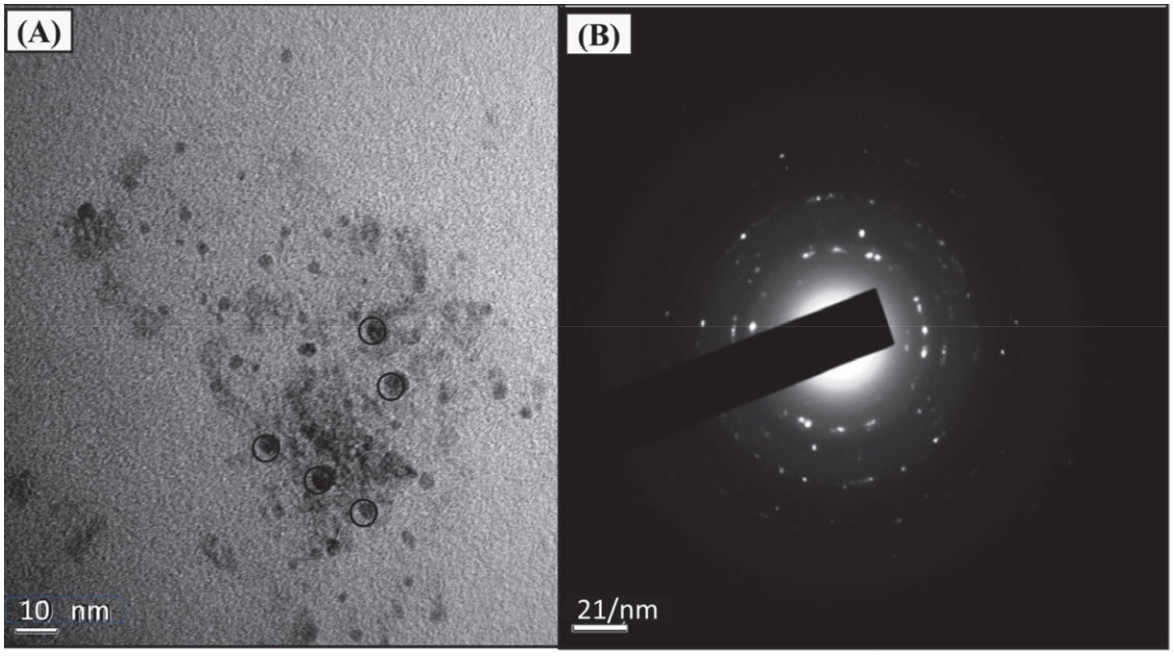

Figure 4: (A) HR-TEM and (B) SAED images of N-GQDs

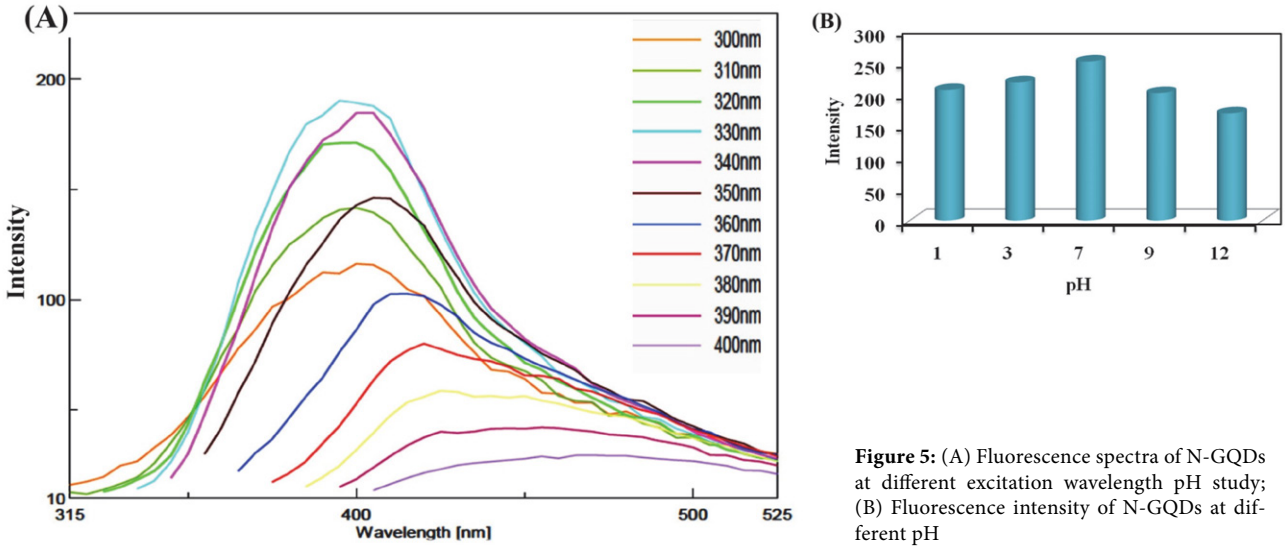

Figure 5: (A) Fluorescence spectra of N-GQDs at different excitation wavelength pH study; (B) Fluorescence intensity of N-GQDs at different pH

thesized N-GQDs were dispersed in a solution of varying pH mainly 1, 3, 7, 9, and 12. The N-GQDs fluorescence intensity was gradually increased with increment in pH of N-GQDs. As a result, the synthesized N-GQDs show the highest fluorescence intensity at neutral pH. On contrary, the fluorescence intensity of N-GQDs was decreased at pH 9 and 12.[29] Therefore, neutral pH was selected for further sensing study of UA. Importantly, the protonation state of N-GQDs could influence fluorescence intensity. In brief, owing to protonation or deprotonation of N-GQDs containing amide and carboxylic functional groups, it gives a carbene-like triplet state that causes changes in photoluminescence.[30–32] The change in pH from 1 to 7 resulted in a high degree of deprotonation of N-GQDs. Subsequently, it generates the deprotonated oxygen atoms and nitrogen atoms on the N-GQDs surface that facilitated the alteration in electron distribution. Hence, the present N-GQDs mediated sensor shows a high fluorescence intensity at the physiological range.[32] At neutral pH, the Quantum yield (QY) of synthesized N-GQDs was found to be 23.78%. Figure 4B concludes that the neutral pH (7) has the highest fluorescence intensity as compared to acidic pH (1, 3) and basic pH (9, 12).

3. 3. Detection of UA using N-GQDs

The fluorescence quenching of N-GQDs was studied by adding different concentrations of UA at 25 °C (Figure 6A). The fluorescence of N-GQDs was observed in the UV cabinet shown in Figure 6B (i and ii). In this study, the fluorescence of N-GQDs (i) gets quenched after UA addition (ii). To study the sensitivity of N-GQDs for UA detection, different concentrations of UA were added to the aqueous solution of N-GQDs followed by measurement of fluorescence intensities. When UA with concentrations ranging from 10 μM to 1000 μM was added to the as-prepared N-GQDs, the fluorescence intensity of N-GQDs was gradually decreased at 245 nm. It presents the relationship of the fluorescent quenching value $\Delta F = F_0 - F^*100$ (F_0 and F are the fluorescence intensities of N-GQDs at 400 nm in the absence and presence of UA, respectively) in varying concentrations of UA (Figure 6C and D). As a result, the ΔF has a good linear relationship with the concentration of UA in the range of 10 μM to 50 μM and 60 μM to 100 μM wherein the linear regression equation was found to be $y = 0.337x + 2.614$ [$R^2 = 0.989$, CI: (0.202, 0.472)] and $y = 0.300x + 8.947$ [$R^2 = 0.981$, CI: (0.165, 0.435)], respectively at 95% of confidence level. It shows both static and dynamic fluorescence quenching in presence of UA[33]. The lowest detection limit of 401.72 ± 0.04 pM (n = 3) was obtained based on a 3.3 σ/Slope (σ: Standard deviation). The comparison of different sensors for the detection of UA is depicted in Table 1. The limit of quantification was found to be 1.217 ± 12 nM, which was calculated based on 10* σ/Slope. The precision of the sensor was measured based on intraday (n = 6) and interday (n = 6) analysis of UA concentration. The percent relative standard deviation (% RSD) was found to be 0.901% and 2.547% for intraday and interday, respectively assuring the high precision for sensing of UA. Importantly, at neutral pH, the fluorescence of N-GQDs was gets quenched sensitively in the existence of UA. It may be because of different possible mechanisms such as static quenching, electron transfer, and an inner filter effect mechanism. Notably, the N-GQDs were exhibited as hydrophilic which may be due to the continuation of surface nitrogen, oxygen functionality. This hydrophilic surface can facilitate the better accessibility of interest analytes in the aqueous media to the 'C' surface. Particularly, it may because of high surface coverage, and more efficient adsorption ability towards interest analyte. This mechanism can alter the surface ion interaction at the edge or on the basal plane of N-GQDs by the modification of surface charge properties. Besides, the occurrence of oxygen functionalities in N-GQDs offers more interaction among the

analyte and carbon surface of N-GQDs.[16] Literature survey divulged that nitrogen doping on nanomaterials surface could change the electrical conductivity and alter the band-gap. Additionally, it can produce electronic defects that can increase the charge transfer ability of nanomaterials. Accordingly, it gives good sensitivity and stability.[34] Herein, doping of nitrogen into GQDs shows high electronegativity and it can transfer lone pair of an electron to electron-deficient molecules.[35] In the present investigation, N-GQDs can transfer two electrons to UA which shows the quenching of fluorescence of N-GQDs.[36] Overall, it is notable that the doping of nitrogen not only enhanced the QY but also improves the chelation ability like oxygen functional groups with the presence of a target marker such as UA that offers the effectual quenching of fluorescence.[14] Taken as a whole, modification of chemical and electronic properties by nitrogen doping into GQDs shows the boosted fluorescence presentation for UA.[33] Herein, more research is necessary to comprehend the quenching mechanics of N-GQDs. For further study, optimizing the doping of nitrogen in the structure of GQDs is essential in N-GQDs-based fluorescent nanosensors for monitoring an analyte.

3. 4. Interference Study

To estimate the selectivity of the proposed method for the determination of UA, the effects of some common metal ions and biomolecules such as NaCl, KCl, $CaCl_2$, $AgNO_3$, lysine, glycine, alanine, glucose, sucrose, and lactose were investigated in triplicates, individually (n = 3). Figure 7 shows the selectivity of N-GQDs towards different interfering substances in presence of the different interfering substances. Herein, common ions and biomolecules had little effect (or slight quenching effect) on the fluorescence of N-GQDs, which was considered to be tolerable. It may be due to available active sites in metal ions and biomolecules that get co-interacted with functionality present on the surface of N-GQDs. Importantly, slight N-GQDs fluorescence quenching effect of different interfering substances was observed that assured the low affinity of N-GQDs towards the selected metal ions and biomolecules.[44] In addition, the fluorescent color alters of N-GQDs upon adding the common ions and biomolecules can be examined by the naked eye below the UV lamp. Moreover, a mixture of numerous metal ions and biomolecules (sample A) had no obvious interference in the de-

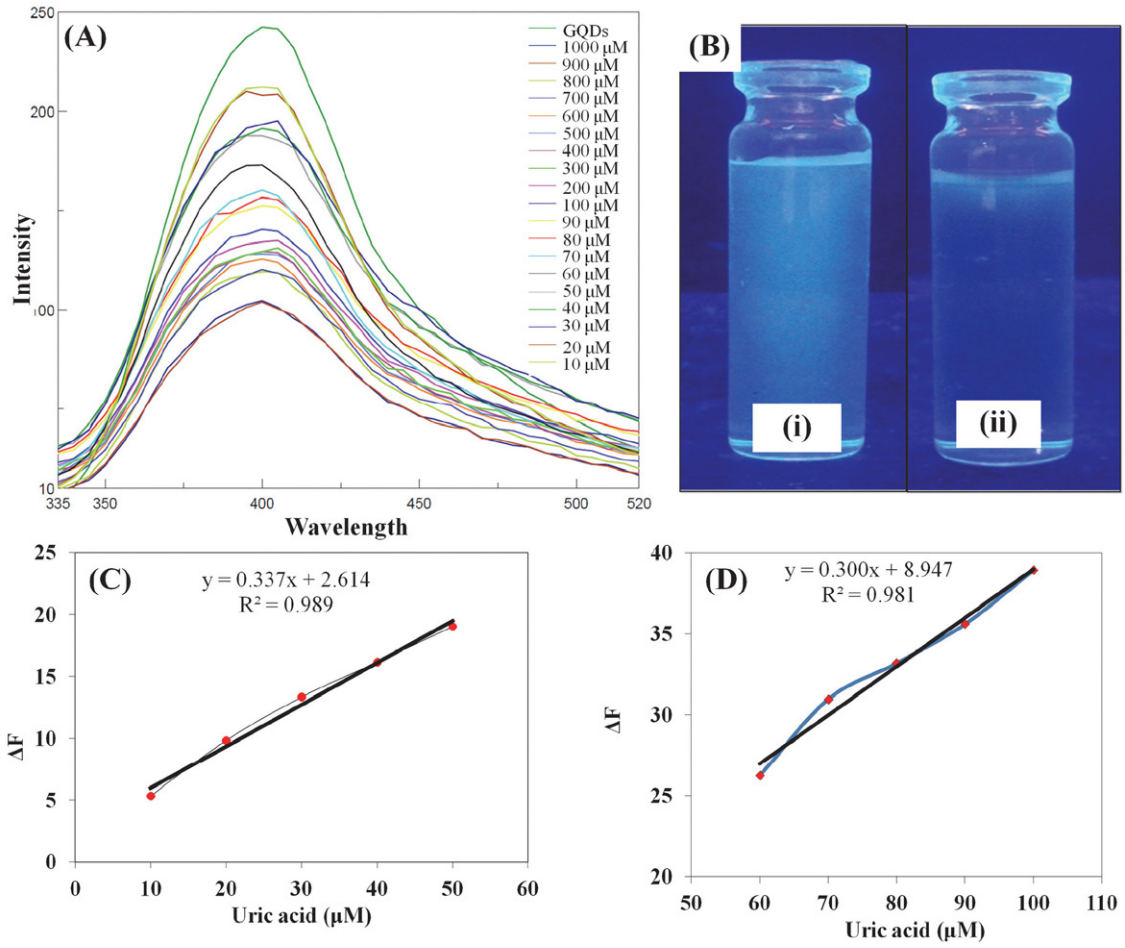

Figure 6: (A) Fluorescence spectra of N-GQDs with different concentrations of UA; (B) Fluorescence of N-GQDs before (i) and after addition of UA (ii); Fluorescence quenching linearity curve [ΔF vs UA concentration ranging from 10 µM to 50 µM (C) and (D) 60 µM to 100 µM, n = 3].

Table 1: Summary of different types of sensors for detection of UA

Sr. No.	Composite	Sensor type	Linearity range	Limit of detection	Ref.
1.	Citrate-capped -PtNPs	Colorimetric	0 mM to 8 mM	4.2 μM	[37]
2.	Poly(dipicolinic acid)/SiO_2@Fe_3O_4	Electrochemical	1.2 μM to 1.8 μM	0.4 μM	[38]
3.	CNCo/GCE	Electrochemical	2 μM to110 μM	0.83 μM	[39]
4.	MoS_2	Electrochemical	10 μM to 400 μM	1.169 μM	[40]
5.	ZnNi@f-MWCNT	Electrochemical	0.2 mM to 1.1 mM	0.51 μM	[41]
6.	r-GO/AuNPs	Electrochemical	10 to 500 μmol dm^{-3}	3.6 μM	[42]
7.	Cu^{2+}@MIL-91(Al:Eu)	Optical	10 μM to 1200 μM	1.6 μM	[43]
8.	N-GQDs	Optical	10 μM to 100 μM	401.72 ± 0.04 pM	Present work

tection of UA. These results demonstrate that the method possesses a good selectivity for the determination of UA. Overall, N-GQDs could be a promising biosensing stage for UA detection in complex samples. The repeatability of the proposed N-GQDs based fluorescent sensor was performed (n = 6) for detection of UA. As a result, it provides the %RSD of 0.802 that confirmed the repeatability of a proposed sensor for the detection of UA. Table 3 shows the summary of analytical characteristics of the N-GQDs based fluorescent biosensor for the determination of UA.

Table 3: Analytical characteristics of the N-GQDs based fluorescent biosensor for determination of UA.

Analytical parameters	Uric acid
	10 μM to 50 μM y = 0.337x + 2.614 [R^2 = 0.989, CI: (0.202, 0.472)] 60 μM to 100 μM y = 0.300x + 8.947 [R^2 = 0.981, CI: (0.165, 0.435)]
Limit of detection (n = 3)	401.72 ± 0.041 pM
Limit of quantification (n = 3)	1.217 ± 12 nM
Precision (% RSD)	
Intraday analysis (n = 6)	0.901 %
Interday analysis (n = 6)	2.547 %
Repeatability (RSD, n = 6)	0.802 %

4. Conclusion

In conclusion, a novel, extremely sensitive, and efficient label-free fluorescence sensing substrate has been developed using N-GQDs. Compared to methods reported in previous studies for N-GQDs synthesis, we have reported a single step, facile, and green synthesis method, which is more economical and less time-consuming. As a result, the prepared N-GQDs were demonstrated excellent optical properties and graphene structure. The as-synthesized N-GQDs emitted strong blue color fluorescence and showed good stability at neutral pH. Afterward, the prepared N-GQDs were utilized for fluorescence detection

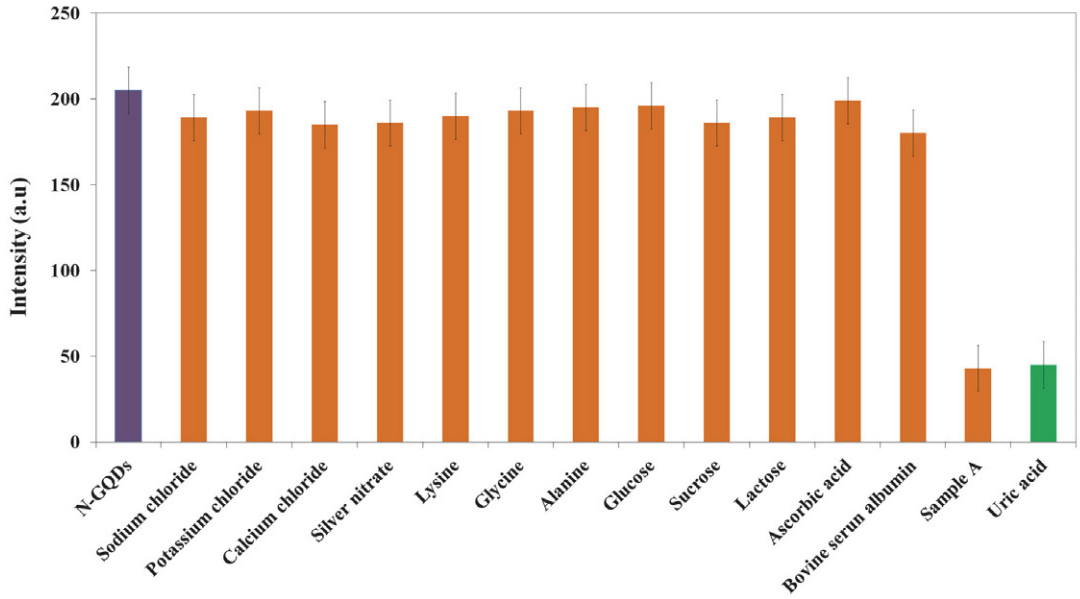

Figure 7: Fluorescence intensity (n = 3) in presence of different ions and biomolecules

of UA. Owing to synergistic static quenching, electron transfer, and inner filter effect mechanisms, the fluorescent N-GQDs nanoprobe exhibited high sensitive detection of UA upto 401.72 ± 0.04 pM. Under the optimum condition, it shows a wide linear response and high selectivity in presence of numerous interfering agents. For further development, there is a major need to control on doping of nitrogen in the structure of GQDs. In a nutshell, N-GQDs can be synthesized from different kinds of waste materials, which are existed in nature. In the upcoming days, the proposed N-GQDs based fluorescent nanoprobe can be used for the determination of UA and other biomarkers in human plasma and urine samples.

Declaration of interest

The authors declare no conflict of interest.

Acknowledgment

Authors are thankful to H. R. Patel Institute of Pharmaceutical Education and Research, Shirpur and Sophisticated Test and Instrumentation Center (STIC), Cochin (Kerala), India, for providing necessary facilities.

5. References

1. J. Du, R. Yue, Z. Yao, F. Jiang, Y. Du, P. Yang and C. Wang, *Colloids Surf A: Physicochem Eng Asp* **2013**, *419*, 94–99 **DOI:**10.1016/j.colsurfa.2012.11.060
2. M. Alam, A. M. Asiri, M. Uddin, M. Islam, M. R. Awual and M. M. Rahman, *New J Chem* **2019**, *43*, 8651–8659. **DOI:**10.1039/C9NJ01287G
3. N. Chauhan and C. S. Pundir, *Anal Biochem* **2011**, *413*, 97–103. **DOI:**10.1016/j.ab.2011.02.007
4. Y. Saito, A. Tanaka, K. Node and Y. Kobayashi, *J Cardiol* **2020**, *78*, 51–57. **DOI:**10.1016/j.jjcc.2020.12.013
5. H. Liu, X. Li, M. Wang, X. Chen and X. Su, *Analytica chimica acta* **2017**, *990*, 150–156. **DOI:**10.1016/j.aca.2017.07.031
6. A. Vernerová, L. K. Krčmová, B. Melichar and F. Švec, *Clin Chem Lab Med (CCLM)* **2020**, *59*,797–812. **DOI:**10.1515/cclm-2020-1533
7. K. Shi and K. K. Shiu, *Electroanalysis: An International Journal Devoted to Fundamental and Practical Aspects of Electroanalysis* **2001**, *13*, 1319–1325. **DOI:**10.1002/1521-4109(200111)13:16<1319::AID-ELAN1319>3.0.CO;2-C
8. J. Lu, Y. Xiong, C. Liao and F. Ye, *Anal Methods* **2015**, *7*, 9894–9899. **DOI:**10.1039/C5AY02240A
9. Q. Li, Y. Qiu, W. Han, Y. Zheng, X. Wang, D. Xiao, M. Mao and Q. Li, *RSC Adv* **2018**, *8*, 25808–25814. **DOI:**10.1039/C7RA12702B
10. R. S. Tade, S. N. Nangare, A. G. Patil, A. Pandey, P. K. Deshmukh, D. R. Patil, T. N. Agrawal, S. Mutalik, A. M. Patil and M. P. More, *Nanotechnology* **2020**, *31*, 292001. **DOI:**10.1088/1361-6528/ab803e
11. L. Ding, H. He, J. Zhou, D. Wang, Q. Nian, S. Li, S. Qian, W. Li, C. Liu, Z. Liang, *Nanotechnology* **2021,** 32(13), 135501. **DOI:**10.1088/1361-6528/abd12a
12. M.W. Abbas, R.A. Soomro, N.H. Kalwar, M. Zahoor, A. Avci, E. Pehlivan, K.R. Hallam, M. Willander, *Microchem J* **2019**, 146, 517–524. **DOI:**10.1016/j.microc.2019.01.034
13. R. S. Tade and P. O. Patil, *ACS Biomater Sci Eng* **2020**, *6*, 5987–6008. **DOI:**10.1021/acsbiomaterials.0c01045
14. J. Ju, R. Zhang, S. He and W. Chen, *Rsc Adv* **2014**, *4*, 52583–52589. **DOI:**10.1039/C4RA10601F
15. K. Kunpatee, S. Traipop, O. Chailapakul, S. Chuanuwatanakul, Sensors and Actuators B: Chemical **2020,** 314, 128059. **DOI:**10.1016/j.snb.2020.128059
16. S. Gu, C.-T. Hsieh, Y.-Y. Tsai, Y. Ashraf Gandomi, S. Yeom, K. D. Kihm, C.-C. Fu and R.-S. Juang, *ACS Appl Nano Mater* **2019**, *2*, 790–798. **DOI:**10.1021/acsanm.8b02010
17. M. Kaur, M. Kaur and V. K. Sharma, *Adv Colloid Interface Sci* **2018**, *259*, 44–64. **DOI:**10.1016/j.cis.2018.07.001
18. Y. Li, Y. Zhao, H. Cheng, Y. Hu, G. Shi, L. Dai and L. Qu, *J Am Chem Soc* **2012**, *134*, 15–18. **DOI:**10.1021/ja206030c
19. G. S. Kumar, R. Roy, D. Sen, U. K. Ghorai, R. Thapa, N. Mazumder, S. Saha and K. K. Chattopadhyay, *Nanoscale* **2014**, *6*, 3384–3391. **DOI:**10.1039/c3nr05376h
20. F. Lu, Y.-h. Zhou, L.-h. Wu, J. Qian, S. Cao, Y.-f. Deng and Y. Chen, *Int J Opt* **2019**, *2019***. DOI:**10.1155/2019/8724320
21. Y. Yang, X. Xiao, X. Xing, Z. Wang, T. Zou, Z. Wang, R. Zhao and Y. Wang, *Mater Res Express* **2019**, *6*, 095615. **DOI:**10.1088/2053-1591/ab3006
22. F. Yang, W. Bao, T. Liu, B. Zhang, S. Huang, W. Yang, Y. Li, N. Li, C. Wang and C. Pan, *Microchim Acta* **2020**, *187*, 1–10. **DOI:**10.1007/s00604-020-04294-8
23. H. M. Kashani, T. Madrakian and A. Afkhami, *New J Chem* **2017**, *41*, 6875–6882. **DOI:**10.1039/C7NJ00262A
24. S.-H. Song, M. Jang, H. Yoon, Y.-H. Cho, S. Jeon, B.-H. Kim, *RSC Adv* **2016**, 6(100), 97990–97994. **DOI:**10.1039/C6RA21651J
25. J. Yu, C. Xu, Z. Tian, Y. Lin and Z. Shi, *New J Chem* **2016**, *40*, 2083–2088. **DOI:**10.1039/C5NJ03252K
26. Z. Yan, X. Qu, Q. Niu, C. Tian, C. Fan and B. Ye, *Anal Methods* **2016**, *8*, 1565–1571. **DOI:**10.1039/C5AY03208C
27. J. Ju, S. Regmi, A. Fu, S. Lim and Q. Liu, *J Biophotonics* **2019**, *12*, e201800367. **DOI:**10.1002/jbio.201800367
28. J. Soleymani, M. Hasanzadeh, M. H. Somi, S. A. Ozkan and A. Jouyban, *Int J Biol Macromol* **2018**, *118*, 1021–1034. **DOI:**10.1016/j.ijbiomac.2018.06.183
29. M. Aghelifar, S. Kimiagar, *Phy Chem Res*. **2018,** 6(2), 237–250.
30. N. R. Mohanty, Kansas State University, **2011**. Web:https://krex.k-state.edu/dspace/handle/2097/9264
31. Q. Li, B. Chen and B. Xing, *Environ Sci Technol* **2017**, *51*, 1364–1376. **DOI:**10.1021/acs.est.6b04178
32. B. Shi, L. Zhang, C. Lan, J. Zhao, Y. Su, and S. Zhao, *Talanta* **2015,** 142, 131–139. **DOI:**10.1016/j.talanta.2015.04.059
33. J. Ju, and W. Chen, *Biosens Bioelectron* **2014**, 58, 219–225. **DOI:**10.1016/j.bios.2014.02.061
34. K. Jindal, M. Tomar and V. Gupta, *Analyst* **2013**, *138*, 4353–4362. **DOI:**10.1039/c3an36695b

35. L. Zhao, H. Li, Y. Xu, H. Liu, T. Zhou, N. Huang, Y. Li, and L. Ding, *Anal Bioanal Chem* **2018** 410(18), 4301–4309. **DOI:**10.1007/s00216-018-1079-6
36. T. S. Thanh, P. T. Qui, N. T. T. Tu, T. T. T. Toan, T. T. B. Hoa, L. V. T. Son, D. M. Nguyen, T. N. Tuyen, and D.Q. Khieu, *J Nanomater* **2021**, 2021. **DOI:**10.1155/2021/9914062
37. M. Ali, M. A. U. Khalid, I. Shah, S. W. Kim, Y. S. Kim, J. H. Lim, and K. H. Choi, *New J Chem* **2019**, 43(20), 7636–7645. **DOI:**10.1039/C9NJ01257E
38. Y. V. M. Reddy, B. Sravani, S. Agarwal, V. K. Gupta, and G. Madhavi, *J Electroanal Chem* **2018,** 820, 168–175. **DOI:**10.1016/j.jelechem.2018.04.059
39. L. Liu, L. Liu, Y. Wang, and B.-C. Ye, Talanta **2019,** 199, 478–484. **DOI:**10.1016/j.talanta.2019.03.008
40. R. Sha, N. Vishnu, and S. Badhulika, *Sens Actuators B Chem* **2019,** 279, 53–60. **DOI:**10.1016/j.snb.2018.09.106
41. A. Savk, B. Özdil, B. Demirkan, M. S. Nas, M. H. Calimli, M. H. Alma, A. M. Asiri, and F. Şen, *Mater Sci Eng C.* **2019,** 99, 248–254. **DOI:**10.1016/j.msec.2019.01.113
42. F. Mazzara, B. Patella, G. Aiello, A. O'Riordan, C. Torino, A. Vilasi, and R. Inguanta, *Electrochim Acta* **2021,** 388, 138652. **DOI:**10.1016/j.electacta.2021.138652
43. X. Lian, and B. Yan, *Inorg.Chem.* **2017,** 56(12), 6802–6808. **DOI:**10.1021/acs.inorgchem.6b03009
44. Y. Wang, S. Zhao, M. Li, W. Li, Y. Zhao, J. Qi, and X. Cui, *J Electroanal Chem* **2017,** 797, 113–120. **DOI:**10.1016/j.jelechem.2017.05.031

Povzetek

Zelene sintetizirane grafenske kvantne pike (GQD) smo dopirali z dušikom, da bi povečali njihove optične značilnosti in sektorje uporabe. V tej preiskavi so bili modri luminiscentni GQD, dopirani z dušikom (N-GQD), sintetizirani z enostopenjsko hidrotermalno sintezo z uporabo prahu lupine tamarinda kot prekurzorja. Ugotovljeno je bilo, da sta velikost delcev in zeta potencial N-GQD 11,40 nm in –35,53 mV. Kvantni izkoristek do 23,78 % je bil dosežen pri valovni dolžini vzbujanja 330 nm pri nevtralnem pH. Fluorescenca se občutljivo zniža v prisotnosti sečne kisline (UA) na podlagi treh mehanizmov: statično dušenje fluorescence, prenos elektronov in mehanizem učinka notranjega filtra. Za UA smo dobili linearno območje od 10 μM do 100 μM z mejo detekcije (LOD) 401,72 ± 0,04 pM. Poleg tega so bili N-GQD selektivni proti UA v prisotnosti kovinskih ionov in biomolekul, kar kaže na njihovo potencialno uporabo za spremljanje UA v kliničnih vzorcih. Skratka, to delo dokazuje, da imajo N-GQD kot zaznavna sonda za prepoznavanje UA določene prednosti pred ostalimi metodami, kot je enostavnost, hitrost analize, pa tudi z družbenoekonomskih aspektov. V prihodnosti je mogoče razcito metodologijo potencialno uporabiti za odkrivanje UA v kliničnih vzorcih.